Revista Mexicana de Astronomía y Astrofísica, 62, 245-249, (2026)

OPEN ACCESS https://doi.org/10.22201/ia.30618649e.2026.62.02.8454

First Seeing Measurements from Ica Solar Station (Perú): An Observatory Located in an Urban Area

N. O. Baella [1], **J. Ricra** [2] **and M. Zegarra-Valles** [2]

[1] *Dirección en Ciencias del Geoespacio, Instituto Geofísico del Perú, Lima, Perú.*
[2] *Instituto Geofísico del Perú, Lima, Perú.*

Keywords: *Site testing, Atmospheric effects, Seeing*

Abstract

The seeing measurements reported in this study were performed at the Ica Solar Station. The observatory is located in an urban area of the city. Observational records were obtained from August to December of 2017. The results show a seeing value of 1.46″, which corresponds to an acceptable sky quality value for the observation station. This is a surprisingly good value considering that it is located on the coast and is adjacent to a large city. It is important to note that the Niño Costero event occurred at the beginning of that year (2017). This makes the measurements particularly interesting for comparison with those from other locations along the Peruvian coast.

Resumen

Se realizaron medidas de *seeing* desde la Estación Solar de Ica. Dicho observatorio se encuentra dentro de una región urbana. Los registros observacionales fueron realizados en el periodo agosto-diciembre del año 2017. Los resultados muestran un valor de seeing de 1.46″correspondiente a un valor aceptable de calidad de cielo para la estación de observación. Un valor sorprendentemente bueno teniendo en cuenta que es un lugar situado en la costa y colindante con una gran ciudad. Es importante indicar que, a principios de dicho año (2017), aconteció el evento del Niño Costero. Esto hace que las mediciones sean particularmente interesantes para ser comparadas con mediciones de otros lugares en la costa peruana.

Corresponding author: Nobar Baella *E-mail address:* nbaella@igp.gob.pe
Received: December 16, 2025 **Accepted:** May 15, 2026

1. Introduction

Unlike space observatories, astronomical images obtained from the ground are affected by the Earth's atmosphere. This distorts stellar images, affecting their position, size, and intensity. Therefore, conducting sky quality studies is of great importance for determining the location of future astronomical observatories. The main criteria that define the sky quality of a given location are atmospheric turbulence (seeing), number of clear nights, atmospheric transparency, and sky background brightness.

In Perú, the first seeing measurements were carried out in 2001 (Baella & Pereyra 2003) at the Huancayo Observatory facilities. The seeing values obtained in this initial study were 3.25″, 2.94″, and 2.71″for the U, B, and V filters, respectively. In subsequent years, additional measurements were performed at the same location. For example, in 2003, Dalmau & Pereyra (2004) reported an average value of 4.16″in the V-band filter. In 2016 and 2017, Ricra (2019) obtained an average value of 2.0″in the R-filter. Using a larger number of measurements, Pereyra et al. (2022) reported an average of 1.92″in the V filter and 1.96″in the R filter for the years 2016 and 2017. Using other measurement techniques, such as Differential Image Motion Monitoring (DIMM), Meza (2014) reported an average seeing value of 1.34″in clear mode.

In addition to the measurements conducted at the Huancayo Observatory, seeing measurements were conducted at other locations in Perú. At the Jicamarca Observatory, Choque & Ishitsuka (2008) reported average seeing values of 3.61″in the V-filter and 3.29″in the B-filter. Meanwhile, at Cerro Sasahuine (Moquegua), Ferradas-Alva et al. (2012) reported an average seeing value of 2.4″in the V-filter and an overall average of 1.8″in the B, V, and R filters.

1.1. Theoretical background

Among the various indicators of sky quality, one of the most important is seeing. This parameter quantifies the effects of atmospheric turbulence on astronomical images. In the absence of an atmosphere, a star does not appear as a point but rather as a diffraction pattern characterized by a bright central disk (Airy disk) surrounded by dark and bright rings (Lombardi 2008). This phenomenon is caused by the diffraction of light at the telescope aperture and is commonly used to determine the theoretical resolution of the telescopes.

The distribution of the star's light on the telescope's CCD is described by the Point Spread Function (PSF). In practice, atmospheric turbulence distorts this ideal pattern, causing the PSF to exhibit a Gaussian profile. The Full Width at Half Maximum (FWHM) of this Gaussian profile is commonly used as an indicator of the level of distortion affecting a star's image and, consequently, serves as a parameter for assessing the sky quality at the observation site.

One of the most widely accepted models that describes the perturbation of the wavefront due to the Earth's atmosphere is the Kolmogorov model (Tatarskii 1961; Kolmogorov 1941). This model states that the FWHM at a given zenith angle (z) is proportional to $\lambda \cdot \sec(z)^{3/5}$, where λ is the wavelength of light. Furthermore, if a plane-parallel atmospheric model is considered, the FWHM at the zenith is related to the FWHM measured at any zenith angle by the following equation:

$$FWHM_{cenit} = \frac{FWHM_{(z)}}{X^{3/5}}, \tag{1}$$

where $X = \sec(z)$

As mentioned, the expression $X = \sec(z)$ is valid for a plane-parallel atmospheric model. However, if we consider the curvature of the atmosphere, the air mass can be expressed using the formula described by Ball (1975).

$$X = \sqrt{y^2 + 2.scale + 1} - y, \tag{2}$$

where $y = scale.cos(z)$ with the scale being the atmospheric scale parameter set at 750 (Allen 1973). The $\cos(z)$ can be calculated from the observer's latitude (ϕ), object's declination (δ), and object's hour angle (H) using the following expression:

$$\cos(z) = \sin(\phi) \cdot \sin(\delta) + \cos(\phi) \cdot \cos(\delta) \cdot \cos(H) \tag{3}$$

2. Observations and Methodology

The observations were made from the Centro de Investigación del Estudio de la Actividad Solar y sus Efectos Sobre la Tierra (CIEASEST) also known as the Ica Solar Station located inside campus of the Luis Gonzaga National University of Ica in Peru. At this station, a Nishimura Cassegrain telescope with an aperture of 60 cm and a focal length of 6000 mm was used to perform observations. The observation site has the following geographic coordinates: South Latitude 14°05′21.34″, West Longitude 75°44′12.49″. Monthly observing outings were scheduled; however, no data were obtained during some of them because of cloudy sky conditions.

The final sample of data acquired for the seeing measurement is shown in Table 1. Col. (1) indicates the name of the object (star) used for the measurements. Col. (2) indicates the date on which the observations were made. Col. (3) indicates the time interval in hours used for the observations. Col. (4) indicates the air mass interval used for the observations. Col. (5) indicates the number of images used in the calculations. The last two columns indicate the mean seeing value for each object; Col. (6) indicates the observed seeing value, and Col. (7) indicates the airmass-corrected seeing values.

The observations for the acquisition of these data were made using a CCD camera (SBIG model ST7) of the anti-blooming type. This camera was coupled to a 0.6 m f/10 Cassegrain telescope (Nishimura Telescope) with an equatorial mount. It is important to mention that the CCD camera was used without a photometric filter wheel. Therefore, all measurements were performed using a clear mode. The plate scale of our telescope-camera system was 0.32″per pixel. This scale corresponds to a field of view (FOV) of 2.7′× 4′.

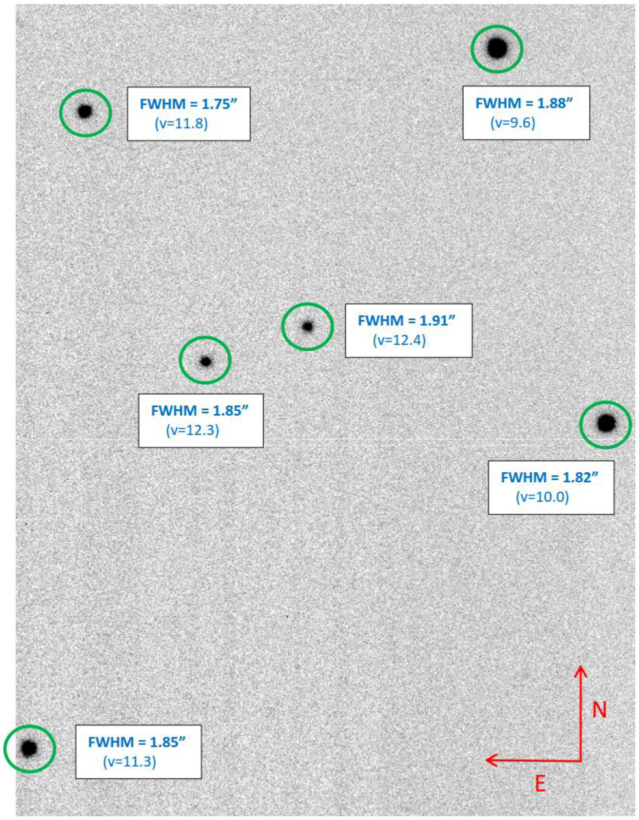

Figure 1. A region of the star cluster M48 (FOV: 2.7′x 4.0′). The mean seeing value for this image was 1.84″with a dispersion of 0.06″. The object had an altitude of 34°at the time of observation. The integration time for this image was 2 seconds.

The exposure times used in our images were between 0.12 s (minimum time allowed by the camera) and 2 s of exposure. All images were dark-corrected.

It is important to mention that the antiblooming characteristic of the camera indicates a nonlinear behavior of the instrument sensitivity near the saturation limit. Therefore, care was taken not to saturate the images by choosing short integration times (between 0.12 and 2 s) for dim objects.

An example of a star field recorded during our missions is shown in Fig. 1. This image was recorded in October and corresponds to the region of the open star cluster M48. Here, we obtained a seeing value of 1.84″with a dispersion of 0.06″(for this field).

Because the FOV is small and taking into account that there is always an inaccuracy between the position to which the telescope is ordered to point (by the corresponding software) and the actual position to which the telescope points, in the last observational missions, care was taken to choose regions of the sky with a higher density of stars. For example, in an open cluster. In particular, the open cluster M48 was chosen for the last two observational missions (see Figure 1). In addition, this cluster presented its highest position above the horizon, almost close to the zenith of the observation site. This allowed the acquisition of data with air mass values that were close to unity.

For example, Fig. 2 shows the results of seeing corrected by air mass for one of the observation nights (December). The maximum (max) and minimum (min) values of the recorded seeing are also indicated in this figure. The corresponding

Table 1. Seeing measurements in the period August-December 2017.

Object (1)	Date (2)	Interval (hours) (3)	Interval (airmass) (4)	N (5)	Seeing Observ. (6)	Airmass correction (7)
HD 215678	2017/08/23	0.4	1.069-1.071	300	1.62 ± 0.37	1.56 ± 0.36
HD 186666	2017/09/26	0.2	2.18-2.40	120	1.51 ± 0.22	0.92 ± 0.13
HD 36922	2017/09/28	1.0	1.47-2.16	79	2.14 ± 0.44	1.52 ± 0.29
HD 215545	2017/10/26	0.6	1.28-1.37	290	1.49 ± 0.31	1.26 ± 0.26
BD-05 2424	2017/10/27	3.4	1.03-2.18	523	1.80 ± 0.35	1.49 ± 0.25
BD-05 2424	2017/12/01	3.6	1.01-1.28	596	1.64 ± 0.29	1.58 ± 0.29

Note: Col. (6) indicate the observed seeing value and Col. (7) the air mass corrected seeing value.

histogram is shown at the bottom of the figure, which includes a normal distribution curve of the measurements. Figure 3 shows a histogram indicating the final mean value obtained from the total number of observations.

2.1. Data reduction

Data processing was initially performed using *MaxIm DL 5* software for conversions from ST7 files to the FIT format. The same program was used to align the images. Afterwards, the tools of the IRAF[1] (Image Reduction and Analysis Facility) software were used for seeing and air mass measurements. All images were flat-field and dark-corrected. The images did not contain universal time (UT) as a parameter in the header; therefore, a small script had to be used to insert this data from the information placed in the date-obs parameter of each image.

The ASTHEDIT task (noao, astutil) was used to calculate the Julian Day (JD) and airmass. Prior to this, the geographical parameters of the observation site were included in the IRAF database. Next, the PSFMEASURE task (noao, obsutil) was used to calculate the Full Width at Half Maximum (FWHM) of the radial profile of the selected star. This value is an indicator of seeing. Finally, the obtained seeing values were corrected for airmass. The corrected seeing values are listed in the last column of Table 1.

3. Analysis

The seeing measurement values are shown in columns (6) and (7) of Table 1. Column (6) indicates the observed mean seeing value, and Column (7) indicates the airmass-corrected mean seeing value. The latter value was obtained using the air mass curvature correction. The dispersion of the mean seeing value was obtained by calculating the sample standard deviation. This was performed for both the observed values and the values for which the air mass correction was applied.

Column (2) indicates the observation dates, which range from August to December 2017. During this period, the presence of clouds in the sky, that is, cloud cover, made data collection difficult. Column (3) indicates the total hours used for data recording for each object in the dataset. A total of 9.2 h of data were recorded. This number of hours can be considered low, but it should be noted that the Peruvian coast in the Ica region has a low number of nights without cloud cover.

In Column (4), the interval of the air mass recorded during the observation is indicated. The values in this column are important because they indicate whether the measurements were made close to the zenith. Of all the objects, the one recorded in December presented air masses closest to the zenith. Column (5) indicates the number of images processed to obtain the seeing value. A total of 1908 images were used and processed.

It is important to note that in the last two observational missions (see the last two rows of Table 1), the open cluster M48 was chosen (Figure 1). This cluster presents its highest point above the horizon, almost close to the zenith of the observation location. The latter allows the acquisition of data with air mass values close to unity.

The final values of the corrected seeing measurements obtained in this study are shown in the final histogram in Fig. 3. An average value of seeing corrected by air mass equal to 1.46±0.33 arcseconds was obtained.

3.1. Seeing measurements for August

August had the highest cloud cover. The best continuous seeing measurement occurred from 00:36 to 00:59 hours (local time) on August 23. During this interval, there was a pause of approximately 8 min owing to the presence of clouds over the observation object. Object HD 215678 has a magnitude V=7.6, with an air mass of 1.07 (altitude of 69 °above the horizon). During the observation, the air mass varied very little; therefore, it can be considered almost constant. A total of 300 images were used to calculate sky quality during the observation session. Each image had an integration period of 0.12 s and was corrected for the dark images. A pause of 8 minutes was observed due to the presence of clouds. Here, we obtained a seeing value of 1.56″with a dispersion of 0.36″.

3.2. Seeing measurements for September

In September, we observed two objects: the first was the star HD 186666 (V=7.6). A total of 120 images were captured and dark corrected. The time interval was 12 min for all measurements. The results are shown in Fig. 3. We obtained a mean corrected seeing of 0.92″. This value is low, but it is important to mention that the uncorrected value shown in Table 1 is 1.51″, which is similar to that of other months. In addition, it has a small observation time interval compared to other missions (October and December). We obtained a mean corrected seeing value of 0.92″with a dispersion of 0.13″.

The second object was the star HD36922 (V=7.75), which has a brightness comparable to that of the first object. Only 79 images were obtained because of the pauses caused by cloud cover. The time interval was one hour. We obtain for this object a seeing value of 1.52″with a dispersion of 0.29″.

[1] https://iraf-community.github.io/doc/beguide.pdf

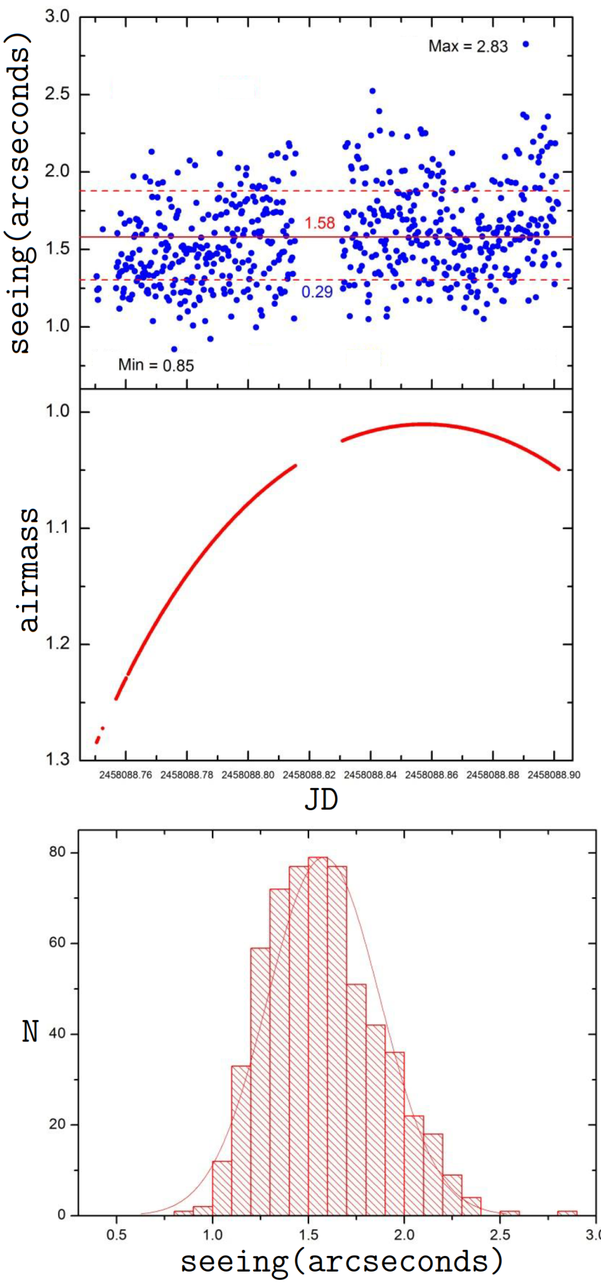

Figure 2. Seeing measurements corrected for air mass (top diagram) obtained on the observation night of 2017/12/01. The maximum (Max) and minimum (Min) seeing values are shown, the airmass interval used and histogram (bottom).

3.3. Seeing measurements for October

In addition, observations were made of two objects: the first was HD 215545 (V=6.5). A total of 290 images were used in this study. The total observation time was 38 min. There were 9 min without data owing to clouds in the observation region. Figure 5 shows the behavior of the seeing during the observation. For this object, we obtained a mean corrected seeing value of 1.26″with a dispersion of 0.26″.

The second observed object was a star in the M48 open cluster. The object was BD-05 2424 (V=9.6). A total of 523 images were obtained and dark-corrected. The total observation duration was 3 h and 24 min.

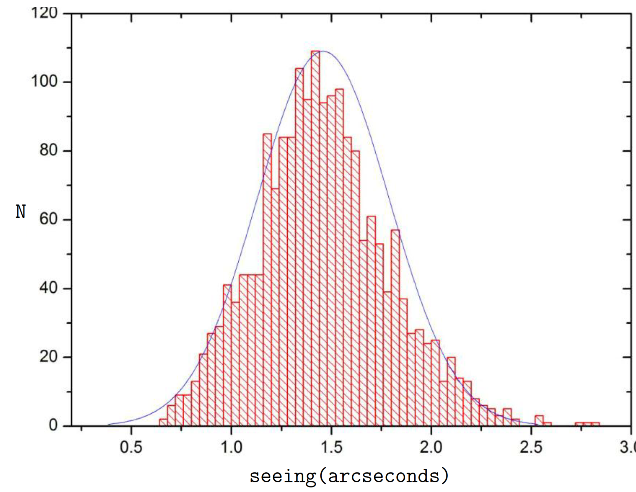

Figure 3. Final histogram of seeing measurements, corrected for air mass, obtained in the period August-December 2017. An average value of seeing corrected for air mass of 1.46″with a dispersion of 0.33″was obtained. The curve with a solid blue line corresponds to a normal distribution fitted to the total sample of seeing records for that period.

Notably, the results obtained showed a low seeing value (1.5 arcseconds) for relatively high airmass values (airmass=2). This can be considered an anomaly because seeing is expected to worsen as the air mass increases. This did not occur during the first few hours. In contrast, as the air mass decreased, the seeing value increased. One possible explanation is the presence of abnormal turbulence above (near the zenith) the telescope on the night of observation. In this sense, the data complement that could be provided by the installation of a future meteorological station near the telescope would help resolve the causes of this behavior. For the second object, we obtained a mean corrected seeing value of 1.49″with a dispersion of 0.25″.

3.4. Seeing measurements for December

Observations were made on the first night of December. At this time, the presence of clouds in the sky decreased, allowing for the recording of a greater number of images. The observed object was also BD-05 2424 (V=9.6). A total of 596 images were obtained. The total observation duration was 3 h and 36 min.

Figure 2 shows the behavior of the seeing as the air mass varies with time. This time, the variation in the seeing was recorded passing through the zenith, with only a small improvement observed after passing through the zenith. The mean corrected seeing value for this observation was 1.58″, with a dispersion of 0.29″.

Once again, the peculiar behavior of the last month was observed. That is, the seeing value tended to decrease with increasing air mass values. Although the effect is smaller here, it is due to the lower value of the air mass interval. This peculiar behavior is less noticeable but exists because it can be observed in the asymmetry of the histogram (Figure 2). As in October, this histogram shows a slight preference for low seeing values. This behavior should be investigated in future studies.

4. Conclusions

In the period August-December 2017, as a result of astronomical seeing measurements made from the Ica Solar Station, an average seeing value equal to 1.46″with a dispersion of 0.33″was obtained. The final histogram (Fig. 3) with seeing measurements already corrected for air mass, presents an acceptable symmetry, considering that all the seeing values recorded in this study were used.

The solid blue curve shown in the diagram (Figure 3) corresponds to a normal distribution adjusted to our total sample of 1908 measurements obtained during the observational missions. Presenting a dispersion of 0.33″The minimum value obtained corresponded to 0.67″. The maximum value recorded was 2.83″.

A peculiar behavior was also found in the relationship between the air mass and the seeing value. At the beginning of the last two observation periods, the seeing value increased as the air mass decreased. This behavior was stronger at the end of October than in that of December. Future installations of meteorological stations close to the telescope could help better understand this phenomenon and determine whether it is only a local behavior or a more extensive one.

Finally, the mean value of 1.46″obtained in this study corresponds to an acceptable sky quality for the observation location. This is a surprisingly good value considering that it is a place located on the coast and adjacent to a large city.

The authors express their gratitude to all the administrative staff of the Faculty of Sciences of Luis Gonzaga National University of Ica and the Ica Solar Station, as well as to Yovanny Buleje Mendoza for providing support to complete this work.

FACILITIES

The observations were made from the Centro de Investigación del Estudio de la Actividad Solar y sus Efectos Sobre la Tierra (CIEASEST), also known as the Ica Solar Station, located inside the campus of the Luis Gonzaga National University of Ica, Perú.

This work was performed using a Nishimura Cassegrain telescope with an aperture of 60 cm and a focal length of 6000 mm. The observation site has the following geographic coordinates: South Latitude 14°05′21.34″, West Longitude 75°44′12.49″.

Data were acquired using a CCD camera (SBIG model ST7) of the antiblooming type, coupled to a 0.6 m f/10 Cassegrain telescope (Nishimura Telescope) with an equatorial mount. The CCD camera was used without a photometric filter wheel, and all measurements were performed in the clear mode.

REFERENCES

Allen, C. W. 1973, Astrophysical quantities, 3rd edn. (London: Athlone Press)

Baella, N., & Pereyra, A. 2003, TECNIA, 13, 15, doi: 10.21754/tecnia.v13i1.480

Ball, J. A. 1975, Algorithms for the HP-45 and HP-35 (Cambridge: Center for Astrophysics, Harvard College Observatory & Smithsonian Astrophysical Observatory)

Choque, E., & Ishitsuka, J. 2008, Compendio de Trabajos de Investigación Realizados por Estudiantes Durante el Año 2007, 9, 9. http://hdl.handle.net/20.500.12816/462

Dalmau, A., & Pereyra, A. 2004, TECNIA, 14, 49

Ferradas-Alva, C., Ferradas-Alva, C., Ferrero, G., et al. 2012, IAUS, 286, 448, doi: 10.1017/S174392131200525X

Kolmogorov, A. 1941, DoSSR, 30, 301

Lombardi, G. 2008, Astronomical Site Testing in the Era of the Extremely Large Telescopes, PhD. Thesis, Department of Physics and Astronomy, University of Bologna, Bologna, Italy

Meza, E. 2014, Implementación el OA-UNI DIMM Seeing Monitor y observaciones de ocultaciones estelares por cuerpos del Sistema Solar desde los Andes Peruanos, Bachelor's thesis, Facultad de Ciencias, Universidad Nacional de Ingeniería, Lima, Perú

Pereyra, A., Tello, J., & Zevallos, M. 2022, JPhCS, 2372, 012001, doi: 10.1088/1742-6596/2372/1/012001

Ricra, J. 2019, Detección y caracterización de planetas extrasolares desde el Perú, Bachelor's Thesis, Facultad de Ciencias, Universidad Nacional de Ingeniería, Lima, Perú

Tatarskii, V. I. 1961, Wave Propagation in Turbulent Medium (New York, USA: McGraw-Hill), 285